British Journal of Pharmacology

DOI:10.1111/j.1476-5381.2011.01600.x
www.brjpharmacol.org

RESEARCH PAPER

# Molecular and functional characterization of the human platelet $Na^+/Ca^{2+}$ exchangers

Diane E Roberts[1], Toshio Matsuda[2] and Ratna Bose[1]

[1]*Department of Pharmacology and Therapeutics; University of Manitoba, Winnipeg, Manitoba, Canada, and* [2]*Laboratory of Medical Pharmacology, Graduate School of Pharmaceutical Sciences, Osaka University, Suita, Osaka, Japan*

**Correspondence**
Dr Ratna Bose, Department of Pharmacology and Therapeutics, University of Manitoba, A311-753 McDermot Avenue, Winnipeg, Manitoba R3E 0W3, Canada. E-mail: rbose@ms.umanitoba.ca

**Keywords**
platelets; $K^+$-dependent $Na^+/Ca^{2+}$ exchanger; $K^+$-independent $Na^+/Ca^{2+}$ exchanger; collagen

**Received**
1 March 2010
**Revised**
20 June 2011
**Accepted**
7 July 2011

## BACKGROUND AND PURPOSE

The $Na^+/Ca^{2+}$ exchanger is a bi-directional transporter that plays an important role in maintaining the concentration of cytosolic $Ca^{2+}$ ($[Ca^{2+}]_i$) of quiescent platelets and increasing it during activation with some, but not all, agonists. There are two classes of $Na^+/Ca^{2+}$ exchangers: $K^+$-independent $Na^+/Ca^{2+}$ exchanger (NCX) and $K^+$-dependent $Na^+/Ca^{2+}$ exchanger (NCKX). Platelets have previously been shown to express NCKX1. However, initial studies from our laboratory suggest that NCX may also play a role in platelet activation. The objective of this study was to determine if the human platelet expresses functional NCXs.

## EXPERIMENTAL APPROACH

RT-PCR, DNA sequencing and Western blot analysis were utilized to characterize the human platelet $Na^+/Ca^{2+}$ exchangers. Their function during quiescence and collagen-induced activation was determined by measuring $[Ca^{2+}]_i$ with calcium-green/fura-red in response to: changes in the $Na^+$ and $K^+$ gradient, NCX pharmacological inhibitors (CBDMB, KB-R7943 and SEA0400) and antibodies specific to extracellular epitopes of the exchangers.

## KEY RESULTS

Human platelets express NCX1.3, NCX3.2 and NCX3.4. The NCXs operate in the $Ca^{2+}$ efflux mode in resting platelets and also during their activation with thrombin but not collagen. Collagen-induced increase in $[Ca^{2+}]_i$ was reduced with the pharmacological inhibitors of NCX (CBDMB, KB-R7943 or SEA0400), anti-NCX1 and anti-NCX3. In contrast, anti-NCKX1 enhanced the collagen-induced increase in $[Ca^{2+}]_i$.

## CONCLUSIONS AND IMPLICATIONS

Human platelets express $K^+$-independent $Na^+/Ca^{2+}$ exchangers NCX1.3, NCX3.2 and NCX3.4. During collagen activation, NCX1 and NCX3 transiently reverse to promote $Ca^{2+}$ influx, whereas NCKX1 continues to operate in the $Ca^{2+}$ efflux mode to reduce $[Ca^{2+}]_i$.

### Abbreviations

$[Ca^{2+}]_i$, concentration of cytosolic calcium; $[K^+]_{ex}$, concentration of extracellular potassium; $[Na^+]_i$, concentration of cytosolic sodium; $Ca^{2+}_i$, cytosolic calcium; DTS, dense tubular system; $IP_3$, inositol 1,4,5-trisphosphate; $K^+_{ex}$, extracellular potassium; NCKX, $K^+$-dependent $Na^+/Ca^{2+}$ exchanger; NCX, $K^+$-independent $Na^+/Ca^{2+}$ exchanger; $PIP_2$, phosphatidylinositol 3,4-bisphosphate; ROC, receptor-operated channel; SOC, store-operated channel; SOCE, store-operated calcium entry

## Introduction

Platelets play a vital role in the haemostatic process through the prevention of blood loss at the site of vascular damage. Injury to the vessel wall exposes circulating platelets to pro-thrombotic elements such as collagen fibres, von Willebrand factor, fibronectin and tissue factor. Collagen is the most thrombogenic component of the subendothelium

(Baumgartner and Haudenschild, 1972) and acts as a substrate for platelet adhesion and activation (Cowan *et al.*, 1981; Morton *et al.*, 1989; Poole and Watson, 1995).

Calcium is an important second messenger in the platelet activation cascade and as such is closely regulated to prevent unwanted thrombosis. Shape change, secretion and aggregation are mediated by an increase in cytosolic $Ca^{2+}$ (Grette, 1962; Born, 1972; Heptinstall, 1976). At rest, platelets maintain the concentration of cytosolic $Ca^{2+}$ ($[Ca^{2+}]_i$) through $Ca^{2+}$ efflux via the plasma membrane $Ca^{2+}$-ATPases and the $Na^+/Ca^{2+}$ exchangers and through uptake of $Ca^{2+}$ into the intracellular stores by the sarco/endoplasmic reticulum $Ca^{2+}$-ATPases (SERCA) 2b and 3 (Rink *et al.*, 1982; Enyedi *et al.*, 1986; Rengasamy *et al.*, 1987; Papp *et al.*, 1991; Wuytack *et al.*, 1994). Platelet $[Ca^{2+}]_i$ is not uniform because of the many homeostatic processes. If maintained for a suitable length of time, resulting transient gradients may influence many important intracellular processes (Alkon and Rasmussen, 1988).

Platelet activation is dependent on an increase in $[Ca^{2+}]_i$, through the release of $Ca^{2+}$ from the intracellular stores and its influx from the extracellular milieu, and is enhanced by secondary mediators generated during platelet activation. Even though the mechanisms involved in the increase in $[Ca^{2+}]_i$ are agonist-specific, there are some common signal transduction pathways. Collagen and thrombin differ in their platelet receptors and initial pathways; however, both activate phospholipase C (PLC) (PLCγ2 and PLCβ, respectively). PLC hydrolysis of phosphatidylinositol 3,4-bisphosphate ($PIP_2$) leads to the formation of inositol 1,4,5-trisphosphate ($IP_3$) and 1,2-diacylglycerol (DAG) (Rittenhouse and Allen, 1982; Watson *et al.*, 1985). $IP_3$ induces the release of calcium from the dense tubular system (DTS) (Authi and Crawford, 1985; Brass and Joseph, 1985), while DAG activates protein kinase C (Nishizuka, 1984). Additionally, $Ca^{2+}$ influx from the extracellular milieu serves as the predominant source of the collagen and thrombin-induced increase in $[Ca^{2+}]_i$ (Jy and Haynes, 1987; Roberts and Bose, 2002). Agonist-induced $Ca^{2+}$ influx can occur through the activation of one or more of the following processes: receptor-operated channels (ROC) activated by the binding of an agonist to a receptor (receptor-operated $Ca^{2+}$ entry), store-operated channels (SOC) activated by the depletion of intracellular stores (store-operated $Ca^{2+}$ entry, SOCE) or the $Na^+/Ca^{2+}$ exchanger functioning in the $Ca^{2+}$ influx mode.

The $Na^+/Ca^{2+}$ exchangers are a family of bi-directional transporters of $Ca^{2+}$. They can modulate both the quiescence and activation of platelets, which makes them an attractive target for the modulation of platelet function. In normal resting cells, the $Na^+/Ca^{2+}$ exchanger functions in the $Ca^{2+}$ efflux mode, thereby contributing to the maintenance of the $10^4$-fold difference in $Ca^{2+}$ concentration across the cell membrane. However, in some pathological states and with certain agonists, the $Na^+/Ca^{2+}$ exchanger's mode of action is reversed, causing an increase in cytosolic $Ca^{2+}$. The $Ca^{2+}$ influx mode of $Na^+/Ca^{2+}$ exchange has been observed in vascular smooth muscle and in platelets in response to salt-sensitive hypertension and diabetes mellitus, respectively (Li *et al.*, 2001; Iwamoto *et al.*, 2004). A $Ca^{2+}$ influx mode of $Na^+/Ca^{2+}$ exchange has also been implicated in collagen (but not thrombin) activation of normal platelets (Roberts and Bose, 2002; Roberts *et al.*, 2004).

There are two classes of $Na^+/Ca^{2+}$ exchangers: the $K^+$-independent $Na^+/Ca^{2+}$ exchanger (NCX) and the $K^+$-dependent $Na^+/Ca^{2+}$ exchanger (NCKX). The NCXs transport $Na^+$ in exchange for $Ca^{2+}$, and the NCKXs transport $Na^+$ in exchange for $Ca^{2+}$ and $K^+$. From functional studies, it has long been known that the human platelet has a $Na^+/Ca^{2+}$ exchanger (Rengasamy *et al.*, 1987; Schaeffer and Blaustein, 1989; Roberts *et al.*, 2004). Previous studies by Kimura *et al.* (1993; 1999) demonstrated that the human platelet contains NCKX1 mRNA and requires $K^+$ for its transport. Initial studies from our laboratory suggested that under certain conditions $K^+$-independent $Na^+/Ca^{2+}$ exchange may also play a role in platelet activation; therefore, in this study, we have investigated and established if the human platelet expresses NCX.

The NCX is a family of electrogenic exchangers whose direction, or mode of action, is determined by the $Na^+$ and $Ca^{2+}$ gradient and the membrane potential of the cell. Three members of the NCX family have been cloned. These are NCX1 (Nicoll *et al.*, 1990), NCX2 (Li *et al.*, 1994) and NCX3 (Nicoll *et al.*, 1996), which are products from three different genes: NCX1 from 2p23p22, NCX2 from 19q13.3 and NCX3 from 14q24.1. NCX1 is expressed in many tissues throughout the body but is present in the largest amounts within the heart. NCX2 and NCX3 are predominantly found in the brain and skeletal muscle (Li *et al.*, 1994; Nicoll *et al.*, 1996). The three exchangers are ~70% identical with respect to their amino acid sequence (Nicoll *et al.*, 1996) and have similar functional properties (Linck *et al.*, 1998). Tissue-specific splice variants have been found for NCX1 and NCX3, but as of yet none for NCX2.

The objective of this study was to determine if the human platelet expresses a $K^+$-independent $Na^+/Ca^{2+}$ exchanger and further characterize it. Although different isoforms of the NCXs have been found in the same tissue (Quednau *et al.*, 1997; Gabellini *et al.*, 2002), rarely have their relative expression levels and function been measured under normal physiological conditions. Our findings indicate that the human platelet expresses three types of the NCX: NCX1.3, NCX3.2 and NCX3.4. The NCXs operate in the $Ca^{2+}$ efflux mode in quiescent and thrombin-activated platelets. In contrast, collagen causes the NCX1 and NCX3 to reverse to a $Ca^{2+}$ influx mode transiently to increase platelet cytosolic $Ca^{2+}$, while the NCKX1 functions in the $Ca^{2+}$ efflux mode to reduce platelet cytosolic $Ca^{2+}$. This study thus helps to establish the identity of the type of $Na^+/Ca^{2+}$ exchangers that are required for activation of human platelets with collagen.

## Methods

### *Materials*

Calcium-sensitive fluorescent dyes calcium-green-AM and fura-red-AM were purchased from Molecular Probes (Eugene, OR). Sodium-sensitive fluorescent dye SBFI-AM was purchased from Molecular Probes. ATP Bioluminescence Assay Kit HS II was purchased from Roche Diagnostics (Mannheim, Germany). Collagen was purchased from Nycomed Arneimittel (Munich, Germany). 5-(4-Chlorobenzyl)-2′,4′-dimethylbenzamil (CBDMB) was obtained from EJ Cragoe (Nacogdoches, TX) and dissolved in dimethyl sulfoxide

(DMSO). 2-[2{4–4-Nitrobenzyloxy)phenyl}ethyl]isothiourea (KB-R7943) was purchased from Tocris Cookson Ltd. (Ellisville, MS, USA) and dissolved in DMSO. 2-[4-[(2,5-Difluorophenyl)-methoxy-phenoxy]-5-ethoxyaniline (SEA0400) was obtained from Dr T Matsuda (synthesized by Taisyo Pharmaceutical Co., Ltd., Saitama, Japan) and dissolved in DMSO. TRIzol® Reagent, ThermoScript™ Reverse Transcriptase, Platinum Taq DNA polymerase and primers were from Invitrogen (Burlington, Ontario, Canada). Rat brain tissue lysate was purchased from ProSci Inc. (Poway, CA). Human retina normal tissue lysate was from GeneTex Inc. (San Antonio, TX). Polyclonal antibodies directed to *N*-terminal extracellular epitopes of NCX1, NCX3 and NCKX1 were obtained from Alpha Diagnostic International (San Antonio, TX). Peroxidase-conjugated secondary antibody was from Jackson Immuno-Research Laboratories (West Grove, PA). Chemicals were from Sigma-Aldrich (Oakville, ON, Canada) unless otherwise stated. The drug and molecular target nomenclature follows BJP's *Guide to Receptors and Channels* (Alexander *et al.*, 2011).

## Ethical approval

Informed consent was obtained from all human volunteers, and the experiments were performed in accordance with the guidelines of the University of Manitoba Research Ethics Board.

## Platelet preparation

Blood was drawn from healthy volunteers into EDTA-containing vacutainer tubes. Platelet-rich plasma was isolated from blood samples by centrifugation at 70 x *g* for 15 min, and then platelets were isolated from the platelet-rich plasma by centrifugation at 800 x *g* for 15 min. Platelet samples were re-suspended in 500 µL of platelet-poor plasma. For the calcium studies, samples were loaded with calcium-sensitive fluorescent dye, calcium-green (10 µM) and fura-red (20 µM) according to previously published techniques (Roberts *et al.*, 2004). For the sodium studies, samples were loaded with sodium-sensitive fluorescent dye SBFI (10 µM) according to previously published techniques (Roberts *et al.*, 2004). Gel filtration with a Sepharose CL-2B (Pharmacia Biotechnology, Piscataway, NJ, USA) column was used to separate platelets from plasma, any remaining white cells and where required extracellular dye. The absence of white cells in the platelet samples used for the molecular studies was confirmed with a haemocytometer and 4′,6-diamidino-2-phenylindole stain. Platelets were eluted in either a $Ca^{2+}$-free HEPES-buffered physiological solution [containing (in mM): 140 NaCl, 4.9 KCl, 1.2 $MgCl_2$, 1.4 $KH_2PO_4$, 5.5 glucose and 20 HEPES (pH 7.4)] or when required a zero potassium $Ca^{2+}$-free HEPES-buffered physiological solution [containing (in mM): 140 NaCl, 1.2 $MgCl_2$, 1.4 $NaH_2PO_4$, 5.5 glucose and 20 HEPES (pH 7.4)], counted in a Coulter counter and adjusted to $2 \times 10^8$ platelets $mL^{-1}$. Where required, the concentration of extracellular potassium ($[K^+]_{ex}$) was adjusted to 5, 25, 45 or 125 mM before each experiment. Where required, *N*-methylglucamine was substituted for NaCl to maintain equal osmolarity.

## Calcium and sodium measurement

The effects of antibodies against extracellular epitopes of NCX1, NCX3 and NCKX1 on the collagen-induced change in cytosolic $Ca^{2+}$ and $Na^+$ were compared with that of non-specific IgG. Aliquots of platelets were incubated for 10 min at 37°C with 25 µg·$mL^{-1}$ rabbit IgG or 25 µg·$mL^{-1}$ anti-NCX1, anti-NCX3 or anti-NCKX1 polyclonal antibodies.

The effects of the NCX inhibitors were evaluated by administering 4 µM CBDMB, 2 µM SEA0400, 5 µM KB-R7943 or the control vehicle (DMSO) to platelets 3 min before their activation with 10 µg·$mL^{-1}$ collagen or 0.5 U·$mL^{-1}$ thrombin.

Aliquots of the platelets were incubated with 1 mM $Ca^{2+}$ at 37°C for 3 min before the test response was performed. Changes in fluorescence were measured at 37°C in a Jasco Inc., Model CAF-110 Ion Analyzer (Easton, MD). The excitation wavelength for $[Ca^{2+}]_i$ measurement was 500 nm, and the emission wavelengths were 540 and 660 nm. The excitation wavelengths for $[Na^+]_i$ measurement were 340 and 380 nm, and the emission wavelengths was 500 nm. $[Ca^{2+}]_i$ and $[Na^+]_i$ were calculated according to previously published formulas (Grynkiewicz *et al.*, 1985; Roberts *et al.*, 2004).

## ATP Measurement

ATP secretion was measured using the ATP Bioluminescence Assay Kit HS II. Before each experiment, 50 µL luciferase reagent was added to aliquots of platelets suspended in $Ca^{2+}$-free HEPES buffer (final reaction volume of 500 µL). The platelets were incubated with 1 mM $Ca^{2+}$ for 3 min before administration of the NCX inhibitors (4 µM CBDMB, 2 µM SEA0400 or 5 µM KB-R7943) or the control vehicle (DMSO), and after an additional 3 min, they were activated with 10 µg·$mL^{-1}$ collagen. The light emitted during each experiment was measured at 37°C in a Jasco Inc., Model CAF-110 Ion Analyzer. The change in luminescence from baseline was used to determine ATP secretion.

## RNA Isolation

Platelets were suspended in TRIzol® Reagent, and total RNA was isolated according to the product insert.

## Reverse transcriptase-PCR

cDNA was synthesized from total RNA (3 µg) by Oligo $(dT)_{20}$ (5 µM) primed reverse transcriptase according to the product insert using ThermoScript™ Reverse Transcriptase. Primers for NCX1 (accession number NM_021097.1) forward 5′-ACATCTGGAGCTCGAGGAAA-3′, reverse 5′-TCCAGCTGT TAGTCCCAACC-3′; NCX2 (accession number XM_0038970) forward 5′-AGGGATTTCAGCTCTGCTACTC-3′, reverse 5′-CA GCATTGACAGAGTCCTTGAG-3′; NCX3 (accession number NM_033262.2) forward 5′-TGAGCAATGTCCGCATAGAG-3′, reverse 5′-TCACCCAATACTGGCTTTCC-3′; and GAPDH (accession number M33197) forward 5′-ATCATCCCTGC CTCTACTGG-3′, reverse 5′-TGGGTGTCGCTGTTGAAGTC-3′ were developed using Primer 3 software (Rozen and Skaletsky, 2000). PCRs were performed in a 50 µL total reaction volume (2 U Platinum Taq DNA polymerase, 200 µM each dNTP, 20 mM Tris–HCl, pH 8.4, 50 mM KCl, 1.5 mM $MgCl_2$ and 200 nM of each appropriate forward and reverse primers in an Eppendorf Mastercycler Gradient). An initial cycle step at 95°C for 5 min was followed by 32 cycles with a 30 s denaturation at 95°C, 20 s annealing with an initial temperature of 70°C and then decreased by 0.5°C for each subsequent cycle, followed by 20 s primer extension at 72°C. An addi-

tional four cycles with an annealing temperature at 60°C was followed by 2 min at 72°C to ensure complete extension. PCR products were visualized by means of a 1.2% (w/v) agarose gel containing ethidium bromide.

PCR products isolated from agarose gel via QIAquick gel extraction kit (Qiagen, Mississauga, Ontario, Canada), were analysed by the University of Calgary DNA Sequencing Laboratory (University Core DNA & Protein Services, Calgary, Alberta, Canada).

## Real-time quantitative PCR

cDNA was synthesized from total RNA (1 μg) by Oligo $(dT)_{20}$ (5 μM) primed reverse transcriptase according to the product insert using ThermoScript™ Reverse Transcriptase. Real-time quantitative PCR was performed in triplicate for each sample in a 25 μL total reaction volume containing: 20 mM Tris–HCl (pH 8.4), 50 mM KCl, 1.5 mM $MgCl_2$, 2% DMSO, 0.5 μL 1:2000 SYBR Green I, 0.5 μL 1:2000 Fluorescein, 0.2 mM dNTPs, 300 nM of each appropriate forward and reverse primer and 0.625 U Platinum Taq DNA polymerase. Primers to NCX1.3 (accession number AF108389) forward 5′-GGCTT CACAATAACAGACGAATATGA-3′, reverse 5′-CAACCACAAG GGCCAGGTTTG-3′; NCX3.2 (accession number AF510501) forward 5′-CGTGGAATATCAGATGTGACAGACAGG-3′, reverse 5′-TCCAGGAATGGGTCCCCACA-3′; NCX3.4 (accession number AF510503) forward 5′-TGCCCGGGGTACAGT CATCG-3′, reverse 5′-TCTGTCACATACAGTTTCATCATTCTT-3′; NCKX1 (accession number AF026132) forward 5′-GCT GCTGCTGCTGGCCTATG-3′, reverse 5′-GTGCTGCGGATG GTGCTGTT-3′; GAPDH (accession number M33197) forward 5′-CGATGCTGGCGCTGAGTACG-3′, reverse 5′-TGGTGCAG GAGGCATTGCTG-3′ were developed using Primer 3 software (Rozen and Skaletsky, 2000). Cycling parameters consisted of an initial step at 95°C for 5 min then 45 cycles with 15 s denaturation at 95°C, 15 s annealing at 60°C and 30 s primer extension at 72°C. The accumulation of fluorescent PCR product was continuously measured using the Bio-Rad iCycler IQ real-time PCR detection system (Mississauga, ON, Canada), followed by melting curve analysis of the PCR products generated. cDNA equivalent to 25, 12.5, 5, 2.5 and 1.25 ng of total RNA was used for each sample in triplicate to determine reaction efficiency. Expression of each isoform of NCX was normalized to GAPDH using the following formula: relative expression = $[(E_{NCX})^{Ct_{NCX}}] / [(E_{GAPDH})^{Ct_{GAPDH}}]$ (Pfaffl, 2001), where $E_{NCX}$ and $E_{GAPDH}$ denote the reaction efficiency of the NCX isoform and GAPDH, respectively. $Ct_{NCX}$ and $Ct_{GAPDH}$ are the mean threshold cycle for the NCX isoform and GAPDH, respectively.

## Western blot analysis

*Platelet preparation.* Isolated platelets were suspended in BRIJ lysis buffer [1% BRIJ 35, 2 μM $Na_2VO_4$, 0.2% SDS, 0.1 M Tris base (pH 7.4), including the CompleteMini® protease inhibitor cocktail] and rocked for 30 min at 4°C.

*Cardiac membrane preparation.* Canine myocardial tissue, used as a NCX1 control, was homogenized in TED buffer (20 mM Tris–HCl, pH 8.0, 10 mM EDTA, 1 mM dithiothreitol and 5 mM phenylmethylsulphonylfluoride). The suspension was centrifuged at 480× *g* for 15 min. The supernatant was then filtered through a cheese cloth, incubated on ice for 15 min with equal volume of 1 M KCl and then centrifuged at 100 000× *g* for 30 min. The pellet obtained was re-suspended in TED and centrifuged at 100 000× *g* for 30 min. The final pellet was then suspended in BRIJ lysis buffer.

*Immunoblotting.* Proteins were transferred to a nitrocellulose membrane (100 V for 90 min) after electrophoretic separation. Non-specific binding sites were blocked, by rocking the nitrocellulose membranes in 5% (w/v) BSA in Tris-buffered saline with 0.05% Tween (TBS-T) at room temperature for 3 h. The membranes were incubated with primary antibodies specific for NCX1 (polyclonal rabbit anti-rat antibody; dilution 1:1000 in 1% BSA TBS-T), NCX3 (polyclonal rabbit anti-rat antibody; dilution 1:1000 in 1% BSA TBS-T) or NCKX1 (polyclonal rabbit anti-human antibody; dilution 1:500 in 1% BSA TBS-T) overnight at 4°C. The nitrocellulose membranes were incubated with peroxidase-conjugated secondary antibody (dilution: 1:5000 in 1% BSA TBS-T). Detection of the peroxidase reaction was performed with the enhanced chemiluminescence assay (Amersham Biosciences, Piscataway, NJ).

## Calculation of rate of decline in $[Ca^{2+}]_i$

Original $Ca^{2+}$ tracings were digitized with a Houston Instruments (Austin, TX, USA) digitizing tablet and the ratios of fluorescence at 540/660 nm were plotted versus time. The ASYST version 3.0 computer system (Mcmillan Software Co., New York, NY) was used to perform compartmental analysis (curve peeling), which resolved the decline in $[Ca^{2+}]_i$ following the collagen-induced peak increase in $[Ca^{2+}]_i$ into two phases with different kinetics. Calcium uptake and efflux was calculated as a % change ($min^{-1}$) with the peak collagen-induced increase in $[Ca^{2+}]_i$ taken as the maximum.

## Statistical analysis

All data are expressed as mean ± SEM. *n* denotes the number of participants (blood donors) from whom the platelets were obtained. ANOVA was used for blocked comparisons. $P < 0.05$ was taken as significant.

# Results

## Evaluation of mRNA expression by PCR

In this study, we have determined if human platelets express the $K^+$-independent type of $Na^+/Ca^{2+}$ exchanger mRNA and identified the specific isoforms. Due to the high degree of sequence homology among the three members of this family of exchangers, primers were chosen to distinguish between not only the three types but also to determine the specific isoforms.

Total RNA was extracted from human platelets, and RT-PCR was performed using primers specific to NCX1, NCX2 and NCX3. This reaction yielded products for NCX1 and NCX3 that could be visualized in an ethidium bromide agarose gel. No bands were observed for NCX2. The NCX1 band of 438 base pairs (bp) was sequenced to confirm its identity as NCX1.3 (Figure 1A). The primers chosen for NCX3 yielded a strong band of 512 bp and a faint band of 412 bp

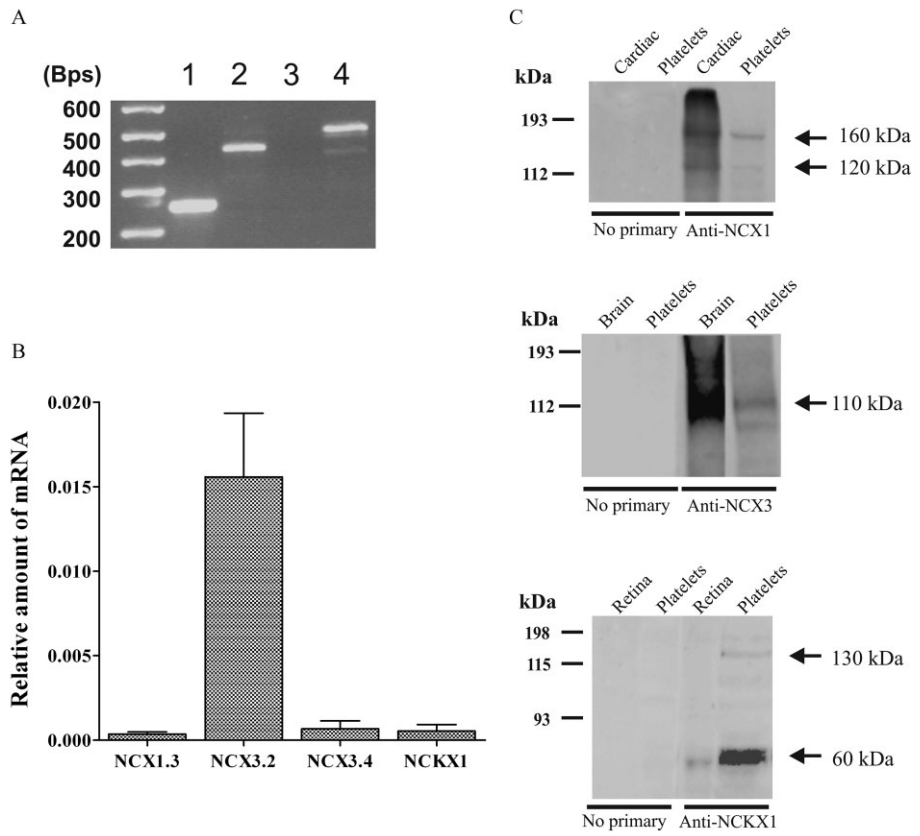


## Figure 1

Characterization of the human platelet $Na^+/Ca^{2+}$ exchangers. (A) NCX mRNA expression by PCR. PCR products from human platelets loaded on a 1.2% agarose gel containing ethidium bromide: GAPDH (1), NCX1 (2), NCX2 (3), NCX3 (4). (B) Real-time quantitative PCR for NCX1.3, NCX3.2, NCX3.4 and NCKX1 expression. Quantitative PCR of cDNA equivalent to 5 ng of total RNA extracted from human platelets was performed by monitoring the continuous accumulation of SYBR Green I fluorescent PCR products using the Bio-Rad iCycler IQ real-time PCR detection system. Each sample was normalized to GAPDH as described in Methods. Data represent the mean values of platelets from four individuals repeated in triplicate. (C) Western blot analysis of the NCX1, NCX3 and NCKX1 expression in human platelets. Ten percent acrylamide gels were loaded with protein from human platelets (35 μg), canine cardiac membranes (20 μg), rat brain (20 μg), human retina (20 μg) and probed with NCX1 polyclonal rabbit anti-rat antibody (1:1000), NCX3 polyclonal rabbit anti-rat antibody (1:1000) and NCKX1 polyclonal rabbit anti-human antibody (1:500).

(Figure 1A). Sequencing of these PCR products confirmed the identity as NCX3.2 and NCX3.4, respectively.

### *Expression of NCX isoforms determined by real-time quantitative PCR*

Real-time quantitative PCR was employed to determine the amount of mRNA expressed in the human platelet for NCX1.3, NCX3.2 and NCX3.4, and how that expression compares with that of NCKX1. NCX3.2 mRNA was found to be the most abundant, approximately 29-fold more than NCX1.3, NCX3.4 and NCKX1 normalized to GAPDH (Figure 1B). Melting curve analysis confirmed that a single homogeneous product was generated for GAPDH, NCX1.3, NCX3.2, NCX3.4 and NCKX1 during the PCR reaction.

### *Identity of NCX proteins by Western blot analysis*

RT-PCR and subsequent sequencing of the PCR products confirmed the presence of NCX1 and NCX3 mRNA. To further determine if human platelets express NCX1, NCX3 and NCKX1 proteins, we performed Western blot analysis. Isolated platelets, cardiac membrane, rat brain total protein lysate and human retina total protein lysate were probed with NCX1, NCX3 or NCKX1 polyclonal antibody to confirm the presence of NCX1, NCX3 and NCKX1 proteins (Figure 1C). The three NCX antibodies did not appear to cross-react with the other types of NCXs. The anti-NCX1 antibody detected a band at ~160 kDa and a faint one at ~120 kDa. NCX3 was detected at ~110 kDa. The anti-NCKX1 antibody showed two bands in platelets, one band at ~130 kDa, the estimated molecular weight for NCKX1, and another band at ~60 kDa. The larger band was absent in the human retina lysate.

### *Role of the $Na^+/Ca^{2+}$ exchanger in resting and activated platelets*

Since the $Na^+/Ca^{2+}$ exchanger's mode of action is dependent on the gradient of the ions it exchanges, alterations to the $Na^+$ gradient was used to establish the role of this exchanger in

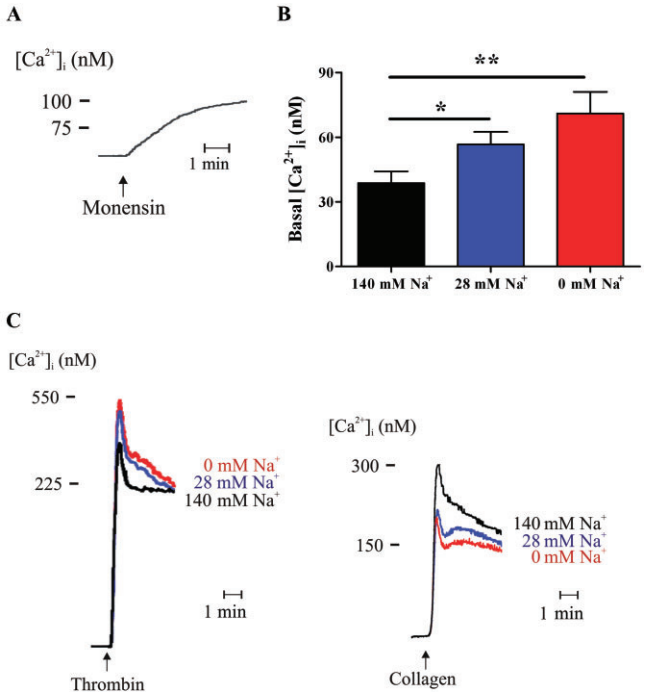


## Figure 2

Role of $Na^+$ in basal and the collagen- and thrombin-induced change in cytosolic calcium. (A) Typical tracing for the change in $[Ca^{2+}]_i$ for platelets suspended in 1 mM $Ca^{2+}$ HEPES physiological buffer following the administration of monensin (10 μM). (B) Basal $[Ca^{2+}]_i$ for platelets suspended in 1 mM $Ca^{2+}$ HEPES physiological buffer containing 140 mM $Na^+$ (normal), 28 mM $Na^+$ (low) or 0 mM $Na^+$ (*$P < 0.05$, $n = 9$; **$P < 0.01$, $n = 9$). (C) Superimposed typical traces for the 0.5 U·mL$^{-1}$ thrombin and 10 μg·mL$^{-1}$ collagen-induced change in $[Ca^{2+}]_i$ for platelets suspended in 1 mM $Ca^{2+}$ HEPES physiological buffer containing 140 mM $Na^+$, 28 mM $Na^+$ or 0 mM $Na^+$.

human platelet function. Administration of the $Na^+$ ionophore monensin (10 μM), to increase $[Na^+]_i$, causes an increase in platelet $[Ca^{2+}]_i$ of 62.1 ± 11.6 nM ($P < 0.005$, $n = 6$) (Figure 2A). Platelets were suspended in buffer containing 140 mM $Na^+$, 28 mM $Na^+$ (low $Na^+$) or 0 mM $Na^+$(no $Na^+$). Low and $Na^+$-free HEPES buffer contained *N*-methyl glucamine to maintain equal osmolarity. Reduction in the concentration of extracellular $Na^+$ results in a significant increase in basal $[Ca^{2+}]_i$, from 38.6 ± 5.4 nM ($n = 9$) for platelets suspended in buffer containing 140 mM $Na^+$ to 56.6 ± 5.8 nM ($P < 0.05$, $n = 9$) in low $Na^+$ buffer and 71.0 ± 10.1 nM ($P < 0.01$, $n = 9$) in $Na^+$-free buffer (Figure 2B). We believe that the difference between these findings and a previously reported study from our laboratory where the reduction in the concentration of extracellular $Na^+$ had no effect on basal $[Ca^{2+}]_i$ is due to a slight difference in the preparation of the platelets for this experiment. If platelets are isolated from the buffer by centrifugation, re-suspended in buffer (containing normal, low or zero $Na^+$) and $[Ca^{2+}]_i$ is immediately measured, we found that there was no significant difference in the basal $[Ca^{2+}]_i$ (Roberts *et al.*, 2004). Gel filtration of the platelets from PPP into buffer containing normal, low or no $Na^+$ results in a delay (~15 min) before $[Ca^{2+}]_i$ is measured. In this case, we believe that enough time has elapsed that a significant change in the basal $[Ca^{2+}]_i$ has occurred. There is, however, no difference between the two methods of preparation for the collagen-induced change in $[Ca^{2+}]_i$. A decrease in the concentration of extracellular $Na^+$ results in a reduction in the collagen-induced change in $[Ca^{2+}]_i$ and an increase in the thrombin-induced change in $[Ca^{2+}]_i$ (Figure 2C). Taken together, these findings illustrate that the $Na^+/Ca^{2+}$ exchanger functions in the $Ca^{2+}$ efflux mode at rest and during thrombin-induced activation of platelets. However, with collagen, the $Na^+/Ca^{2+}$ exchanger reverses to a $Ca^{2+}$ influx mode, and the reduction in the collagen-induced $[Ca^{2+}]_i$ in low and no $Na^+$ buffer is due to reduced $Na^+$ influx triggering $Na^+/Ca^{2+}$ exchange reversal.

### *Role of the $K^+$-dependent and -independent $Na^+/Ca^{2+}$ exchangers in the collagen-induced increase in $[Ca^{2+}]_i$*

The platelet agonist collagen has been shown to induce the reversal of the $Na^+/Ca^{2+}$ exchanger, resulting in the influx of $Ca^{2+}$ into the cytosol and subsequently platelet aggregation (Roberts and Bose, 2002; Roberts *et al.*, 2004). However, because the platelets express both $K^+$-dependent and -independent $Na^+/Ca^{2+}$ exchangers, we wanted to determine what role they play in the collagen-induced increases in $[Ca^{2+}]_i$.

### *Role of the $K^+$-independent $Na^+/Ca^{2+}$ exchangers in the collagen-induced increase in $[Ca^{2+}]_i$*

Pharmacological inhibitors of the $K^+$-independent $Na^+/Ca^{2+}$ exchangers (NCXs), CBDMB, KB-R7943 and SEA0400, were used to elucidate the role of these exchangers in the collagen-induced change in $[Ca^{2+}]_i$. CBDMB and KB-R7943 have been shown to decrease the collagen-induced change in $[Ca^{2+}]_i$ in a dose-dependent manner and have a $ED_{50}$ of 4.7 ± 1.1 and 35.1 ± 4.8 μM, respectively (Roberts and Bose, 2002; Roberts *et al.*, 2004). SEA0400 was also found to decrease the collagen-induced change in $[Ca^{2+}]_i$ in a dose-dependent manner with a $ED_{50}$ of 2.2 ± 0.5 μM ($n = 4$). The concentrations of CBDMB (4 μM) and SEA0400 (2 μM) used in this study was based on the $ED_{50}$, whereas 5 μM KB-R7943 was used to avoid possible inhibition of other channels that has been observed in other cells with higher concentrations of this drug (Takano *et al.*, 2001; Tanaka *et al.*, 2002). Administration of the NCX inhibitor CBDMB, the $Ca^{2+}$ influx mode-selective NCX1 inhibitor SEA0400 (Matsuda *et al.*, 2001), or the $Ca^{2+}$ influx mode-selective NCX3 inhibitor KB-R7943 reduced the collagen-induced increase in $[Ca^{2+}]_i$ (Figure 3A and Table 1). Whereas with thrombin, which does not reverse the function of the $Na^{2+}/Ca^{2+}$ exchangers, CBDMB and KB-R7943 increased the thrombin-induced change in $[Ca^{2+}]_i$ and SEA0400 had no effect (Figure 3B and Table 1). KB-R7943 is referred to as a $Ca^{2+}$ influx mode-selective inhibitor because the dose required to inhibit $Ca^{2+}$ influx is much less than the dose that inhibits $Ca^{2+}$ efflux in cardiac myocytes (Iwamoto *et al.*, 1996). In our studies with platelets, the increase in the thrombin-induced $[Ca^{2+}]_i$ with 5 μM KB-R7943 indicates that it was able to inhibit the thrombin-induced $Ca^{2+}$ efflux. In another series of experiments, the effect of NCX inhibition on the collagen-induced change in $[Ca^{2+}]_i$ was studied in the absence of extracellular $Ca^{2+}$. It confirmed that the collagen-

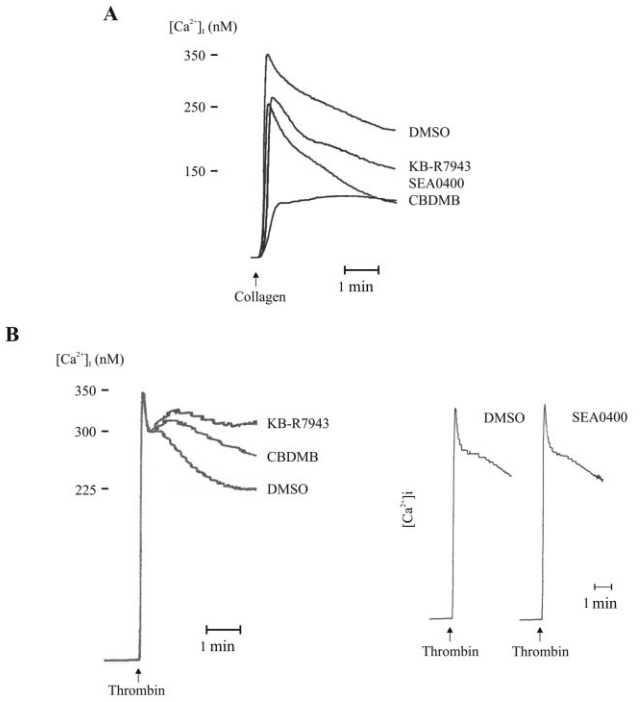


## Figure 3

Role of the K$^+$-independent Na$^+$/Ca$^{2+}$ exchangers in the collagen and thrombin-induced change in cytosolic calcium. (A) Superimposed typical tracings of the collagen-induced change in $[Ca^{2+}]_i$ for platelets administered CBDMB (4 μM), SEA0400 (2 μM), KB-R7943 (5 μM) or vehicle control (DMSO) 3 min before their activation with 10 μg·mL$^{-1}$ collagen. (B) Typical tracings of the thrombin-induced change in $[Ca^{2+}]_i$ for platelets administered CBDMB (4 μM), SEA0400 (2 μM), KB-R7943 (5 μM) or vehicle control (DMSO) 3 min before their activation with 0.5 U·mL$^{-1}$ thrombin.

## Table 1

Role of the K$^+$-independent Na$^+$/Ca$^{2+}$ exchangers in the collagen and thrombin-induced change in cytosolic calcium

| Treatment | % change in $[Ca^{2+}]_i$ | SEM | Sample size | Significance |
|---|---|---|---|---|
| Collagen | | | | |
| DMSO | 100 | 0 | 5 | |
| CBDMB | 26.1 | 4.0 | 5 | $P < 0.0001$ |
| KB-R7943 | 83.7 | 3.7 | 5 | $P < 0.05$ |
| SEA0400 | 54.8 | 2.1 | 5 | $P < 0.001$ |
| Thrombin | | | | |
| DMSO | 100 | 0 | 4 | |
| CBDMB | 124.7 | 6.8 | 4 | $P < 0.05$ |
| KB-R7943 | 160.3 | 12.3 | 4 | $P < 0.05$ |

Average % change in platelet $[Ca^{2+}]_i$ measured 3 min following their activation with collagen (10 μg·mL$^{-1}$) or thrombin (0.5 U·mL$^{-1}$) for platelets administered CBDMB (4 μM), SEA0400 (2 μM), KB-R7943 (5 μM) or vehicle control (DMSO).

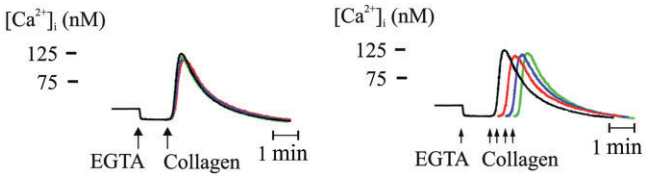


## Figure 4

Effect of the K$^+$-independent Na$^+$/Ca$^{2+}$ exchange inhibitors on the collagen-induced release of intracellular calcium. Superimposed (left) and staggered (right) typical traces for the 10 μg·mL$^{-1}$ collagen-induced change in $[Ca^{2+}]_i$ in the absence of extracellular Ca$^{2+}$ achieved through its chelation with 5 mM EGTA and administered vehicle control (DMSO, black), CBDMB (4 μM, red), KB-R7943 (5 μM, blue) or SEA0400 (2 μM, green) 3 min before their activation with collagen.

## Table 2

Effect of the K$^+$-independent Na$^+$/Ca$^{2+}$ exchange inhibitors on the collagen-induced release of intracellular calcium

| Treatment | Collagen-induced % change in $[Ca^{2+}]_i$ | SEM | *n* | Significance |
|---|---|---|---|---|
| Zero extracellular Ca$^{2+}$ | | | | |
| DMSO | 24.5 | 7.1 | 4 | ns |
| CBDMB | 19.0 | 2.9 | 4 | ns |
| KB-R7943 | 24.2 | 0.8 | 4 | ns |
| SEA0400 | 22.5 | 1.2 | 4 | ns |

The average % change in $[Ca^{2+}]_i$ measured 3 min following activation with collagen (10 μg·mL$^{-1}$) for platelets suspended in 0 mM extracellular Ca$^{2+}$ achieved with EGTA (5 mM) and administered vehicle control (DMSO), CBDMB (4 μM), KB-R7943 (5 μM) or SEA0400 (2 μM) 3 min prior to their activation with collagen. The collagen-induced change in $[Ca^{2+}]_i$ for platelets suspended in buffer with 1 mM Ca$^{2+}$ was taken as 100%. ns, not significant.

induced release of Ca$^{2+}$ from the intracellular stores was unaffected by the NCX inhibitors at the concentrations used in this study (Figure 4 and Table 2).

The effects of SEA0400 and KB-R7943 were further evaluated by subtracting the collagen-induced change in $[Ca^{2+}]_i$ for platelets administered SEA0400 or KB-R7943 from their vehicle control (DMSO) response. The results show a transient activation of the Ca$^{2+}$ influx mode for NCX1 and NCX3, as observed by the initial increase in $[Ca^{2+}]_i$ that declines to near baseline levels after 5 min (Figure 5). The lack of a complete return to baseline indicates that some exchangers are still functioning in the Ca$^{2+}$ influx mode, possibly due to relative proximity to the source of Na$^+$ influx that triggers reversal. CBDMB inhibits NCX functioning in both the Ca$^{2+}$ influx and efflux mode; this inference was drawn by subtracting the effect of CBDMB on the collagen-induced change in $[Ca^{2+}]_i$ from the vehicle control (DMSO) to show the change in $[Ca^{2+}]_i$ that is due to the NCX. In this case, the initial

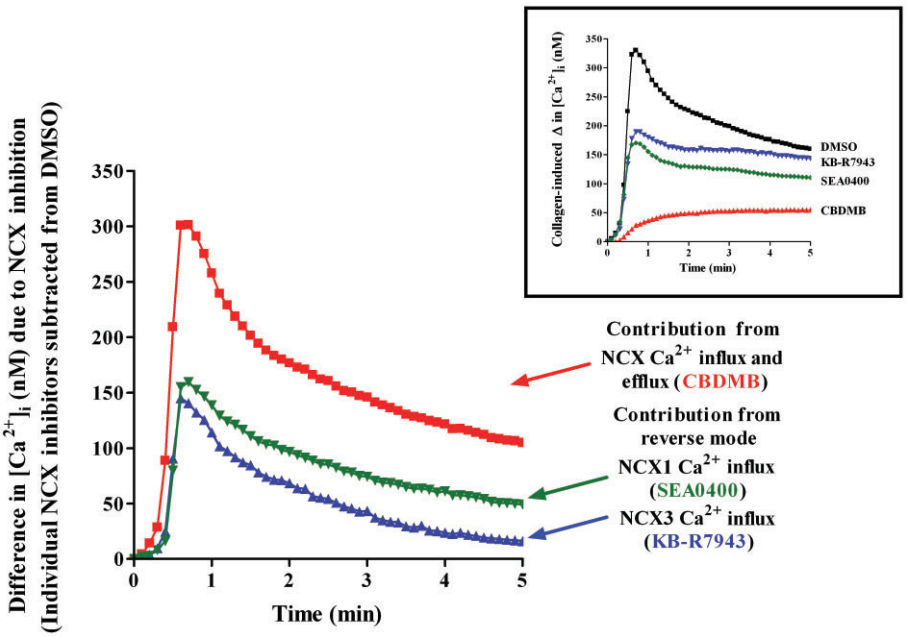


## Figure 5

Contribution of $K^+$-independent $Na^+/Ca^{2+}$ exchangers to the collagen-induced calcium influx and efflux. Superimposed typical tracings of the collagen-induced change in $[Ca^{2+}]_i$ for platelets administered the NCX inhibitor CBDMB (4 μM), the reverse mode selective NCX1 inhibitor SEA0400 (2 μM) and the reverse mode-selective NCX3 inhibitor KB-R7943 (5 μM) compared with vehicle control (DMSO) 3 min before their activation with 10 $\mu g \cdot mL^{-1}$ collagen (insert). The contribution of the NCXs to $[Ca^{2+}]_i$ was calculated by subtracting the collagen-induced change in $[Ca^{2+}]_i$ for the respective inhibitors from their DMSO control: $Ca^{2+}$ influx and efflux through the NCXs blocked by CBDMB; $Ca^{2+}$ influx through NCX1 and NCX3 blocked by SEA0400 and KB-R7943, respectively. The typical tracings shown here were similar for platelets from four other individuals.

increase in $[Ca^{2+}]_i$, due to reversal of NCX1 and NCX3, is followed by a decline in $[Ca^{2+}]_i$ that plateaus and does not return to baseline (Figure 5) as observed with SEA0400 and KB-R7943. Taken together, the data indicate that the decline in $[Ca^{2+}]_i$ observed for platelets administered SEA0400 or KB-R7943 is most likely due to these inhibitors only affecting the collagen-induced $Ca^{2+}$ influx mode and not the efflux mode as observed with CBDMB, which leads to a higher $[Ca^{2+}]_i$ in the second phase compared with the other NCX inhibitors. Although other interpretations for this effect are possible, such as an effect on the intracellular $Ca^{2+}$ stores, this has been ruled out because of the lack of effect of these drugs on the cytosolic $Ca^{2+}$ profile in $Ca^{2+}$-free media.

### *Effects of CBDMB, KB-R7943 and SEA0400 on dense granule secretion and store depleted activated $Ca^{2+}$ entry*

Collagen-induced dense granule secretion was measured using an ATP bioluminescence assay to measure ATP secretion. There was no change in ATP secretion following the addition of the NCX inhibitors. Furthermore, the collagen-induced rate and amount of ATP secretion was not significantly changed by 4 μM CBDMB (98.4 ± 2.1%, $n$ = 4), 5 μM KB-R7943 (95.4 ± 6.2%, $n$ = 4) or 2 μM SEA0400 (100.4 ± 2.8%, $n$ = 4) when compared with DMSO (Figure 6A and B).

KB-R7943 (50 μM) has been shown to reduce the $Ca^{2+}$ influx pathway activated by the depletion of intracellular stores (SOCE) using thapsigargin (Harper *et al.*, 2009). Consequently, the effects of the NCX inhibitors at the concentrations used in this study on $Ca^{2+}$ entry following thapsigargin were tested (Figure 6C). The average $Ca^{2+}$ entry in thapsigargin-treated platelets administered 4 μM CBDMB (226.2 ± 41 nM, $n$ = 5), 5 μM KB-R7943 (280.9 ± 44 nM, $n$ = 5) and 2 μM SEA0400 (231.4 ± 29 nM, $n$ = 5) was not significantly different compared with DMSO (273.1 ± 35 nM, $n$ = 5) measured 2 min following the addition of 1 mM $CaCl_2$ (Figure 6D).

From these findings, we concluded that the NCX inhibitors (CBDMB, KB-R7943 and SEA0400) at the concentrations used in this study had no significant effect on the release of stored $Ca^{2+}$ or SOCE.

### *Role of the $K^+$-dependent $Na^+/Ca^{2+}$ exchangers in the collagen-induced increase in $[Ca^{2+}]_i$*

Since there are no good pharmacological inhibitors available for NCKX1, changes to the $K^+$ gradient were used to elucidate the role of NCKX1 in the collagen-induced changes in $[Ca^{2+}]_i$. Under normal resting physiological conditions, the platelet $Na^+/Ca^{2+}$ exchangers operate in the $Ca^{2+}$ efflux mode. The presence of 0, 5 or 25 mM $[K^+]_{ex}$ caused no significant change in the basal $[Ca^{2+}]_i$, 39.0 ± 2.4, 39.8 ± 2.3 and 41.3 ± 2.2 nM, respectively (NS, $n$ = 6; Figure 7A). The change in $[Ca^{2+}]_i$, measured 3 min following the administration of collagen, was not significantly different for platelets suspended in

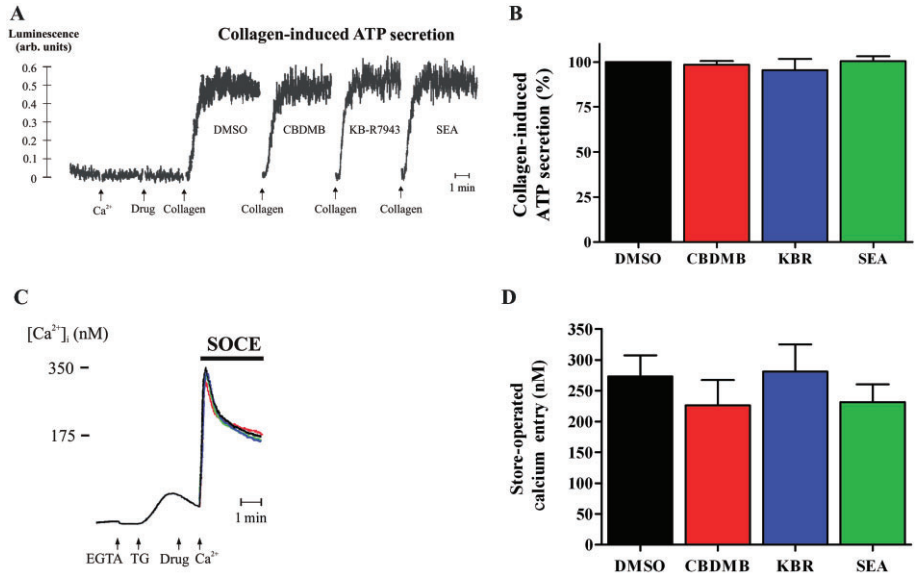


## Figure 6

The effect of the NCX inhibitors on ATP secretion and $Ca^{2+}$ entry. (A) Typical tracings of the collagen-induced change in ATP secretion for platelets administered CBDMB (4 μM), SEA0400 (2 μM), KB-R7943 (5 μM) or vehicle control (DMSO) 3 min before their activation with 10 $\mu g \cdot mL^{-1}$ collagen. (B) Average % change in the collagen-induced ATP secretion for platelets administered CBDMB (4 μM), SEA0400 (2 μM) or KB-R7943 (5 μM) compared with DMSO measured 2.5 min following collagen (NS, $n = 4$). (C) Superimposed typical traces of the effect CBDMB (4 μM, red), SEA0400 (2 μM, green), KB-R7943 (5 μM, blue) or vehicle control (DMSO, black) has on $Ca^{2+}$ entry following thapsigargin. Platelets were administered 400 μM EGTA to chelate extracellular $Ca^{2+}$ and then 200 nM thapsigargin to release stored $Ca^{2+}$. CBDMB, SEA0400, KB-R7943 or DMSO was added 1 min before the addition of 1 mM $CaCl_2$. (D) Average $Ca^{2+}$ entry measured 2 min following the addition of 1 mM $CaCl_2$ for platelets administered CBDMB (4 μM), SEA0400 (2 μM), KB-R7943 (5 μM) or DMSO (NS, $n = 5$).

buffer containing 0 mM $K^+$ (155.3 ± 17 nM, $n = 6$), 5 mM $K^+$ (167.2 ± 21 nM, $n = 6$) or 25 mM $K^+$ (145.3 ± 25 nM, $n = 6$) (Figure 7B and C). From this, we concluded that the $K^+$-dependent $Na^+/Ca^{2+}$ exchanger is not reversed to a $Ca^{2+}$ influx mode following the administration of collagen.

The thermodynamics of NCKX1 and the large $K^+$ gradient would favour the exchanger to function in the $Ca^{2+}$ efflux mode. In order to further characterize the role of NCKX1 during the collagen activation of platelets, the rate of removal of $Ca^{2+}$ from cytosol was measured in response to an increase in $[K^+]_{ex}$ to 45 and 125 mM. There are two phases to the decline in $[Ca^{2+}]_i$ following the collagen-induced peak increase in $[Ca^{2+}]_i$, which can be measured via compartmental analysis (Figure 8A and B). The first phase was not significantly affected by alterations to the $[K^+]_{ex}$ (data not shown). In the second phase, the rate of $Ca^{2+}$ efflux was reduced when $[K^+]_{ex}$ was increased to 45 mM (by 24.3 ± 19%, NS, $n = 5$) and 125 mM (by 84.2 ± 28%, $P < 0.05$, $n = 5$; Figure 8C and D) as compared with control $[K^+]_{ex}$ of 5 mM.

### *Role of the $Na^+/Ca^{2+}$ exchanger isoforms in the collagen-induced increase in $[Ca^{2+}]_i$*

The functional role that various isoforms of the $Na^+/Ca^{2+}$ exchangers play during the collagen activation of human platelets was additionally supported by the use of antibodies for the exchangers. The antibodies are specific to extracellular epitopes of NCX1, NCX3 and NCKX1 and were not found to cross react. There was no significant difference in the collagen-induced increase in $[Ca^{2+}]_i$ for platelets incubated for 10 min at 37°C with either non-specific IgG (rabbit IgG) or control vehicle (Figure 9A, insert). Incubation of platelet samples with antibodies against either NCX1 or NCX3 reduced the collagen-induced increase in $[Ca^{2+}]_i$. Conversely, antibodies to NCKX1 increased the collagen-induced increase in $[Ca^{2+}]_i$ (Figure 9A). The effects of the antibodies on the collagen-induced change in $[Ca^{2+}]_i$ could be prevented by pre-incubation of the antibodies with their specific antigen (Figure 9A, insert). Compared with non-specific IgG, the collagen-induced increase $[Ca^{2+}]_i$ was reduced by 15.7 ± 6.5% (NS, $n = 5$) when platelets were pretreated with the antibody against NCX1 and by 31.5 ± 8.1% ($P < 0.05$, $n = 5$) when pretreated with the antibody against NCX3 (Figure 9B). The collagen-induced change in $[Ca^{2+}]_i$ was increased by 52.9 ± 8.8% ($P < 0.001$, $n = 5$) for platelets pretreated with the antibody against NCKX1 as compared with non-specific IgG (Figure 9B).

The time line for the contribution of the inhibitors and hence individual exchangers to the collagen-induced increase in $[Ca^{2+}]_i$ was determined by subtracting the effect measured for platelets pretreated with antibodies to the exchangers (NCX1, NCX3 or NCKX1) from those administered non-specific IgG. The collagen-induced calcium influx through NCX1 and NCX3 is transient in nature, and the initial rapid increase in $[Ca^{2+}]_i$ is followed by a gradual decline in $[Ca^{2+}]_i$ (Figure 9C), whereas the NCKX1 functions in the $Ca^{2+}$ efflux mode to reduce $[Ca^{2+}]_i$ and reaches a steady state following the administration of collagen (Figure 9C).

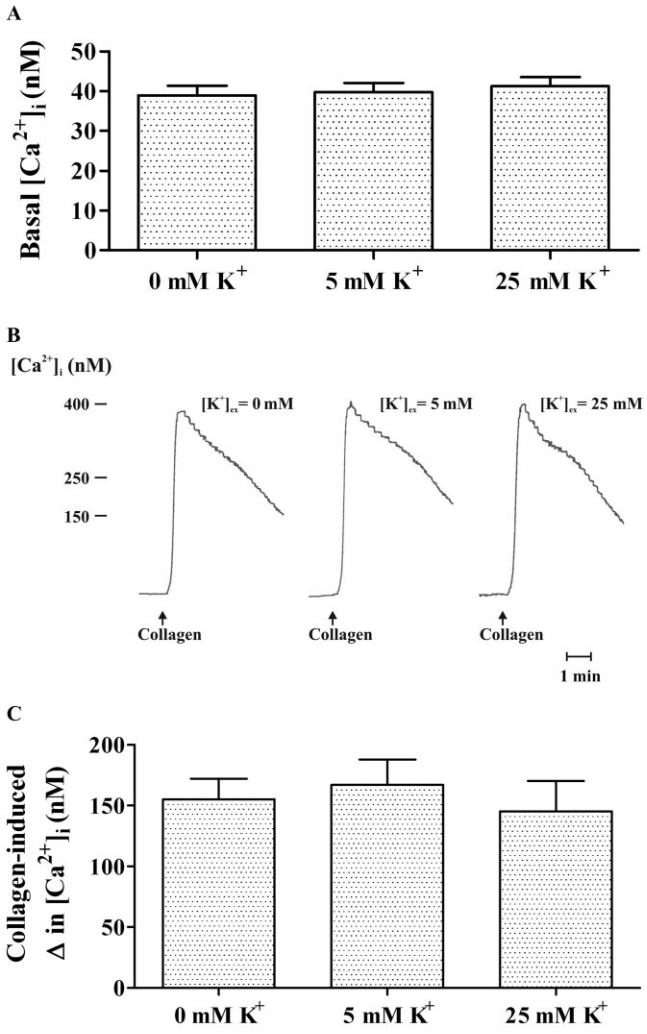


## Figure 7

Collagen-induced change in $[Ca^{2+}]_i$ in the presence and absence of extracellular potassium. (A) Basal $[Ca^{2+}]_i$ for platelets suspended in 1 mM $Ca^{2+}$ HEPES physiological buffer containing 0 mM $K^+$, 5 mM $K^+$ (normal) or 25 mM $K^+$ (NS, $n = 6$). (B) Typical traces for the 10 $\mu g \cdot mL^{-1}$ collagen-induced change in $[Ca^{2+}]_i$ for platelets suspended in 1 mM $Ca^{2+}$ HEPES physiological buffer containing 0 mM $K^+$, 5 mM $K^+$ (normal) or 25 mM $K^+$. (C) Collagen-induced change in $[Ca^{2+}]_i$ measured 3 min following the administration of 10 $\mu g \cdot mL^{-1}$ collagen to platelets suspended in 1 mM $Ca^{2+}$ HEPES physiological buffer containing 0 mM $K^+$, 5 mM $K^+$ (normal) or 25 mM $K^+$ (NS, $n = 6$).

### *Role of the $Na^+/Ca^{2+}$ exchanger isoforms in the collagen-induced change in $[Na^+]_i$*

Collagen-induced increase in $[Ca^{2+}]_i$ through reversal of the $Na^+/Ca^{2+}$ exchanger to a $Ca^{2+}$ influx mode is dependent on an increase in $[Na^+]_i$. The increased $[Na^+]_i$ is exchanged for extracellular $Ca^{2+}$, resulting in an increase $[Ca^{2+}]_i$. We have previously shown that collagen induces an increase in $[Na^+]_i$ (Roberts *et al.*, 2004). To further establish the role of the $Na^+/Ca^{2+}$ exchangers in the collagen-induced increase in $[Ca^{2+}]_i$, we tested the effect blocking the $Na^+/Ca^{2+}$ exchanger has on the collagen-induced change in $[Na^+]_i$. A buildup of cytosolic $Na^+$ with $Na^+/Ca^{2+}$ exchange inhibition indicates that the exchanger is functioning in the $Na^+$ efflux and $Ca^{2+}$ influx mode. Conversely, a reduction in cytosolic $Na^+$ with $Na^+/Ca^{2+}$ exchange inhibition indicates that the exchanger is functioning in the $Na^+$ influx and $Ca^{2+}$ efflux mode. Antibodies to the $Na^+/Ca^{2+}$ exchangers were used because other agents used for inhibiting NCXs quench SBFI fluorescence, for example CBDMB (unpublished observation from our laboratory) and KB-R7943 (Harper and Sage, 2007b). There was no significant difference in the collagen-induced increase in $[Na^+]_i$ for platelets incubated with either non-specific IgG or control vehicle. Compared with non-specific IgG, the collagen-induced change in $[Na^+]_i$ was increased by 36.1 ± 8.0% ($P < 0.01$, $n = 4$) and 58.6 ± 12.1% ($P < 0.01$, $n = 4$) for platelets pretreated with the antibody against NCX1 and NCX3, respectively (Figure 10). The collagen-induced change in $[Na^+]_i$ was reduced 26.2 ± 6.5% ($P < 0.05$, $n = 4$) for platelets pretreated with the antibody against NCKX1 as compared with non-specific IgG (Figure 10). The effects of the antibodies against NCX1, NCX3 and NCKX1 could be prevented by the prior incubation with their specific antigen. From these results, we conclude that in response to collagen, $Na^+$ builds up in the platelet when NCX1 and NCX3 are inhibited, and less $Na^+$ enters when NCKX1 is blocked. This further supports our conclusion that collagen induces the reversal of NCX1 and NCX3, while NCKX1 continues to operate in the $Ca^{2+}$ efflux mode.

## Discussion

The $Na^+/Ca^{2+}$ exchangers are bi-directional transporters of $Ca^{2+}$ and can have a dual role in platelet activation or maintenance of quiescence. It has been previously reported that the human platelet expresses a $K^+$-dependent $Na^+/Ca^{2+}$ exchanger (Kimura *et al.*, 1993; 1999). We show here that in addition to the $K^+$-dependent $Na^+/Ca^{2+}$ exchanger, three isoforms of $K^+$-independent $Na^+/Ca^{2+}$ exchangers are expressed in the human platelet: NCX1.3, NCX3.2 and NCX3.4. As shown here, and previously presented in abstract form (Roberts *et al.*, 2005), NCX1 and NCX3 can be detected by Western blot analysis. The presence of NCX3 has also been recently reported by other laboratories, however, they were unable to detect NCX1 (Lewandrowski *et al.*, 2009; Harper *et al.*, 2010). The reason for this discrepancy is unclear at this time. We have been able to detect NCX1 with anti-NCX1 antibody from either Alpha Diagnostic International or provided by Dr KD Philipson, UCLA. Given the discovery of both $K^+$-dependent and -independent $Na^+/Ca^{2+}$ exchangers and our previous findings that $Ca^{2+}$ influx via $Na^+/Ca^{2+}$ exchanger is the predominant source of the collagen-induced increase in $[Ca^{2+}]_i$ (Roberts and Bose, 2002; Roberts *et al.*, 2004), we sought to determine which $Na^+/Ca^{2+}$ exchangers are involved in collagen-induced platelet activation.

Platelet activation is dependent on an increase in $[Ca^{2+}]_i$, from the release of stored $Ca^{2+}$ and its influx from the extracellular milieu. We have shown that collagen-induced increase in $[Ca^{2+}]_i$ is dependent on the $Na^+$ gradient and reduced by inhibitors of the $Na^+/Ca^{2+}$ exchanger since they are functioning in the $Ca^{2+}$ influx mode. This is unlike the effects of NCX inhibitors observed during thrombin-induced platelet activation (Li *et al.*, 2001 and as shown here). It has

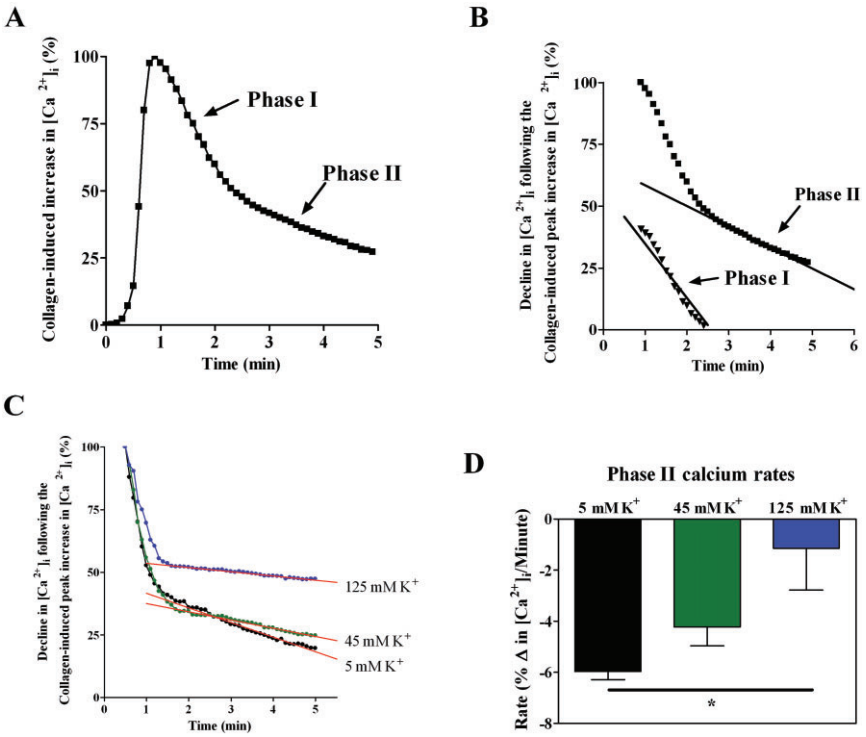


## Figure 8

Effects of high extracellular $K^+$ on the rate of decrease in $[Ca^{2+}]_i$. (A) Shows a typical 10 μg·mL$^{-1}$ collagen-induced change in $[Ca^{2+}]_i$ for platelets suspended in HEPES physiological buffer containing 1 mM $Ca^{2+}$ and 5 mM $K^+$ (normal control). Curve peeling resolved the rate of decline in $[Ca^{2+}]_i$, after the peak increase in $[Ca^{2+}]_i$ with collagen (peak taken as 100%), into two phases with two rates of decline (slopes). In (B), data points are the 'peeled' data points from (A) for the phase one decline after the contribution from the other phase was deducted. The slope of the best-fit lines 1 and 2 are the respective rates for phases 1 and 2. (C) Superimposed typical traces for the decline in $[Ca^{2+}]_i$ from the peak following the administration of 10 μg·mL$^{-1}$ collagen. Platelets were suspended in 1 mM $Ca^{2+}$ HEPES physiological buffer containing 5 mM $K^+$ (normal), 45 mM $K^+$ or 125 mM $K^+$. Their corresponding best fit line, in red, illustrates the phase two rate of decline in $[Ca^{2+}]_i$ for the three treatment groups. (D) Rate of the phase two decline in $[Ca^{2+}]_i$ for platelets suspended in 1 mM $Ca^{2+}$ HEPES physiological buffer containing 5 mM $K^+$(normal), 45 mM $K^+$ or 125 mM $K^+$ and activated with 10 μg·mL$^{-1}$ collagen (*$P < 0.05$, $n = 5$).

been reported that following $Ca^{2+}$ release with thapsigargin, $Ca^{2+}$ entry occurs through SOC and the $Na^+/Ca^{2+}$ exchanger operating in the $Ca^{2+}$ influx mode (Harper and Sage, 2007a). However, it was subsequently reported that the NCX inhibitors reduced SOCE by reducing dense granule secretion instead of inhibiting the $Na^+/Ca^{2+}$ exchanger (Harper *et al.*, 2009). At the concentrations used in our study, the NCX inhibitors had no effect on $Ca^{2+}$ entry through SOC (Figure 6C and D), the collagen-induced release of intracellular $Ca^{2+}$ (Figure 4) or dense granule secretion (Figure 6A and B). SOCE occurs during platelet activation with collagen and thrombin. If these inhibitors were acting on SOCE instead of the $Na^+/Ca^{2+}$ exchangers, then they should have the same effect on the collagen and thrombin-induced change in $[Ca^{2+}]_i$. ADP and ATP are secreted from the dense granules and act through a positive feedback mechanism potentiating platelet activation. The P2X receptor is a ligand-gated non-selective cation channel that when activated results in $Ca^{2+}$ and $Na^+$ influx at a ratio of 4:1 (Valera *et al.*, 1994). ATP activates the P2X receptor and can increase $[Ca^{2+}]_i$ directly via the influx of $Ca^{2+}$, or indirectly through the reversal of the $Na^+/Ca^{2+}$ exchanger as seen in airway smooth muscle cells (Flores-Soto *et al.*, 2011). In platelets, the P2X1 receptor has been implicated in low-dose collagen activation but not with concentrations greater than 2.5 μg·mL$^{-1}$ (Oury *et al.*, 2002; 2003; Hechler *et al.*, 2003; Fung *et al.*, 2005), probably due to the activation of additional positive feedback pathways. Thus, it is unlikely that direct or indirect $Ca^{2+}$ influx via P2X1 is involved in the collagen-induced change in $[Ca^{2+}]_i$ observed here. It is more likely that $Na^+$ influx is through a receptor-operated channel or more specifically the transient receptor potential channels (Gudermann *et al.*, 2004), which have been shown to co-localize with NCX1 and trigger the latter into a $Ca^{2+}$ influx mode (Rosker *et al.*, 2004; Eder *et al.*, 2007).

The $Na^+/Ca^{2+}$ exchangers operate in the $Ca^{2+}$ efflux mode in resting platelets (Figure 11A) and during their activation with thrombin but not collagen. Collagen-induced $Ca^{2+}$ influx through the $Na^+/Ca^{2+}$ exchanger is dependent on an increase in $[Na^+]_i$. Cytosolic $Na^+$ is exchanged for extracellular $Ca^{2+}$, resulting in an increase $[Ca^{2+}]_i$; therefore, $[Na^+]_i$ increase must precede $Ca^{2+}$ influx. We believe that the slow increase in $[Na^+]_i$ when measured with SBFI, a weak fluorescent probe that measures the global change in $Na^+$, is because a sufficient amount of $Na^+$ must diffuse fully into the platelet cytosol to be detected. Meanwhile, $Na^+$ influx is occurring at the membrane near the $Na^+/Ca^{2+}$ exchanger where it is exchanged for

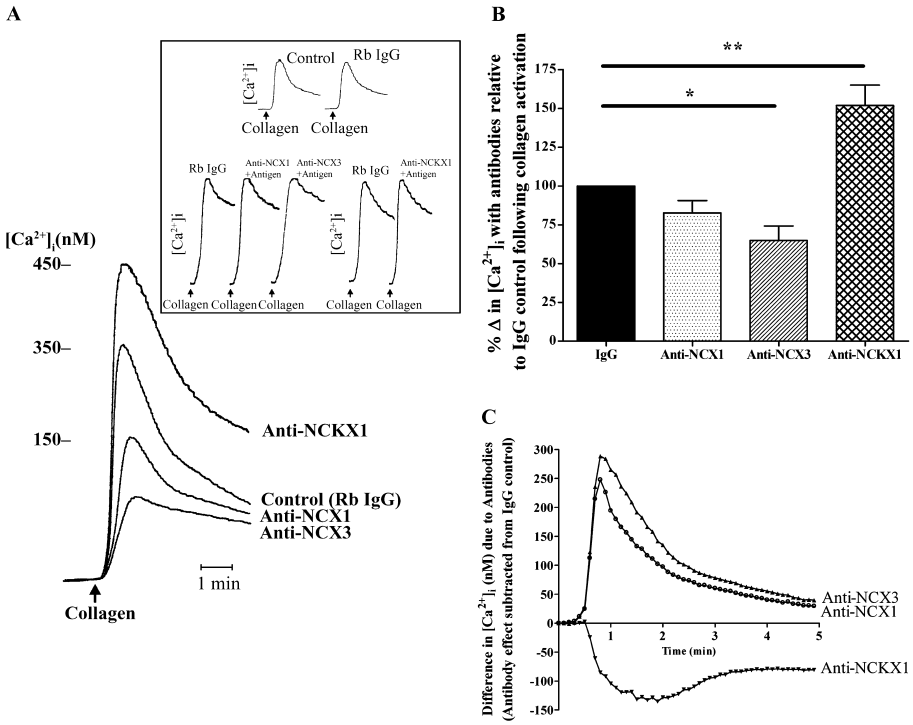


## Figure 9

Effect of $Na^+/Ca^{2+}$ exchanger antibodies on the collagen-induced change in $[Ca^{2+}]_i$. (A) Superimposed typical tracings for the 10 μg·mL$^{-1}$ collagen-induced change in $[Ca^{2+}]_i$ for platelets incubated with Rb IgG, anti-NCX1, anti-NCX3 or anti-NCKX1. (Insert) Typical trace for the collagen-induced $[Ca^{2+}]_i$ for platelets incubated with control vehicle, non-specific IgG, anti-NCX1, anti-NCX3 or anti-NCKX1 and their respective antigens. (B) The collagen-induced change in $[Ca^{2+}]_i$ measured 3 min following the administration of 10 μg·mL$^{-1}$ collagen to platelets incubated with anti-NCX1, anti-NCX3 or anti-NCKX1 compared with those incubated with non-specific IgG expressed as % (*$P < 0.05$, $n = 5$; **$P < 0.001$, $n = 5$). (C) Collagen-induced change in $[Ca^{2+}]_i$ contributed by the three $Na^+/Ca^{2+}$ exchangers was calculated for platelets pretreated with anti-NCX1, anti-NCX3 or anti-NCKX1 and subtracted from those pretreated with Rb IgG.

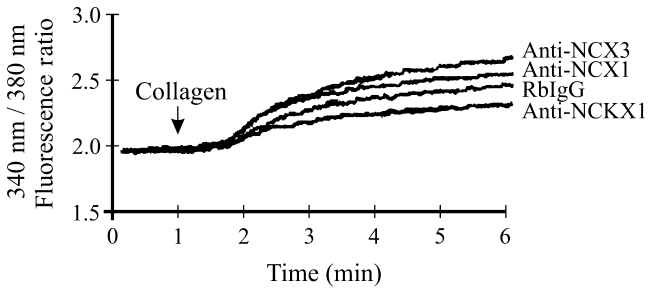


## Figure 10

Effect of $Na^+/Ca^{2+}$ exchanger antibodies on the collagen-induced change in $[Na^+]_i$. Superimposed typical tracings for the 10 μg·mL$^{-1}$ collagen-induced change in $[Na^+]_i$ for platelets incubated with Rb IgG, anti-NCX1, anti-NCX3 or anti-NCKX1.

$Ca^{2+}$. Collagen-induced increase in $[Na^+]_i$ (Roberts *et al.*, 2004 and as shown here) is enhanced by blocking $K^+$-independent $Na^+/Ca^{2+}$ exchangers NCX1 and NCX3, and reduced when the $K^+$-dependent $Na^+/Ca^{2+}$ exchanger NCKX1 is inhibited. This further supports our conclusion that collagen induces the reversal of NCX1 and NCX3, while NCKX1 continues to operate in the $Ca^{2+}$ efflux mode (Figure 11B).

It is difficult to establish whether the collagen-induced $Ca^{2+}$ influx is predominately through NCX1 or NCX3. From the results using anti-NCX1 and anti-NCX3, it would appear that the collagen-induced $Ca^{2+}$ influx occurs largely by NCX3 and to some extent by NCX1. Whereas SEA0400 reduced the collagen-induced change in $[Ca^{2+}]_i$ more than KB-R7943. However, while SEA0400 was used at its $ED_{50}$, KB-R7943 was administered at a dose less than a third of its $ED_{50}$ for human platelets to avoid possible inhibition of other channels that has been observed in other cells with higher concentrations of this drug (Takano *et al.*, 2001; Tanaka *et al.*, 2002; Roberts *et al.*, 2004). The conclusions in this manuscript regarding the qualitative roles of the different $K^+$-independent $Na^+/Ca^{2+}$ exchangers during collagen activation will not be changed if the NCXs are partially or fully inhibited. Furthermore, it is highly unlikely that three structurally diverse inhibitors (SEA0400, KB-R7943, NCX1 and NCX3 antibodies) would give us such comparable changes in $Ca^{2+}$ if they were working through different mechanisms or molecules other than the NCXs.

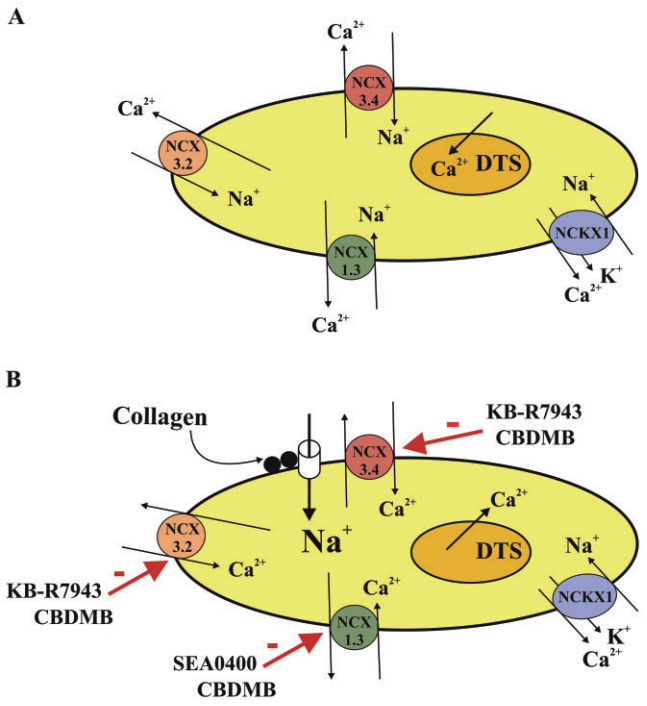


## Figure 11

Schematic diagram for the proposed roles of NCX1, NCX3 and NCKX1. (A) Calcium movement via NCX1, NCX3 and NCKX1, and the dense tubular system (DTS) in the human platelets at rest. (B) The proposed roles of NCX1, NCX3 and NCKX1 in human platelets in response to collagen, and the inhibitors that influence them.

The NCKX was not anticipated to play a role in collagen-induced platelet activation since $[Ca^{2+}]_i$ showed no dependence on $K^+_{ex}$ (0–25 mM). However, not only is NCKX1 activated, it functions in the forward mode, thus blunting the increase in $[Ca^{2+}]_i$. Given the large $K^+$ gradient favouring forward mode, it is not until $K^+_{ex}$ is increased to 45 or 125 mM that changes in NCKX1 function become apparent in the reduced rate of $Ca^{2+}$ efflux in the second phase of the platelets' response to collagen. We believe that changes in NCKX1 function, if any, in response to changes in $K^+_{ex}$ between 0 and 25 mM were masked by other exchangers and ion pumps in the platelet membrane. Absence of $K^+_{ex}$ would enhance the forward mode of NCKX1 and also inhibit the $Na^+/K^+$-ATPase, resulting in an increase in $[Na^+]_i$ enhancing the reverse mode of the NCXs after initial decrease in the forward mode. Increasing $K^+_{ex}$ to 25 mM would theoretically reduce forward-mode NCKX1 and increase $Na^+/K^+$-ATPase removal of cytosolic $Na^+$, thereby reducing reverse mode of the NCXs. The $Na^+$ influx induced by collagen would be anticipated to cause platelet membrane depolarization; however, no change in the membrane potential has been reported (MacIntyre and Rink, 1982). It is possible that the net movement of $K^+$ and $Na^+$ in opposite directions is sufficient to prevent depolarization. MacIntyre and Rink (1982) also found little or no change in membrane potential caused by thrombin and ADP, respectively, which has been subsequently shown to cause membrane depolarization of 6–8 mV (Pipili, 1985). To our knowledge, no other studies have measured the effect of collagen on platelet membrane potential.

There is a fundamental difference between NCX and NCKX that can explain how it is possible for them to display opposite modes of action in response to collagen. NCX operates with a stoichiometry of $3Na^+$ to $1Ca^{2+}$ (Reeves and Hale, 1984; Hinata and Kimura, 2004), whereas the NCKX transports $4Na^+$ for $1Ca^{2+}$ and $1K^+$ (Cervetto *et al.*, 1989; Schnetkamp *et al.*, 1989). Consequently, a larger increase in $[Na^+]_i$ and possibly a decrease in the $K^+$ gradient would be required to reverse NCKX. Their difference in the function during activation may cause different microenvironments within the platelet that is necessary for shape changes and other functions.

Increased $[Ca^{2+}]_i$ precedes platelet activation, making the mechanisms that regulate it important therapeutic targets for the manipulation of platelet function. In some pathological states such as diabetes mellitus, the $Na^+/Ca^{2+}$ exchanger operates in the $Ca^{2+}$ influx mode, increasing $[Ca^{2+}]_i$, thus making platelets prone to form unwanted micro-thrombi (Li *et al.*, 2001). In this instance, preventing $Ca^{2+}$ influx through the $Na^+/Ca^{2+}$ exchanger may be a potential method to prevent the formation of micro-thrombi. However, to be an effective therapeutic intervention, the identity of the target must be well defined.

In conclusion, human platelets express $K^+$-dependent and independent $Na^+/Ca^{2+}$ exchangers. During collagen activation, the $K^+$-independent $Na^+/Ca^{2+}$ exchangers, NCX1 and NCX3, transiently reverse to a $Ca^{2+}$ influx mode, increasing $[Ca^{2+}]_i$, whereas the $K^+$-dependent $Na^+/Ca^{2+}$ exchanger NCKX1 continues to operate in the $Ca^{2+}$ efflux mode.

## Acknowledgements

We would like to thank the following: Molly Pind for assistance with qPCR studies; Dr EJ Cragoe for providing us with CBDMB; Dr KD Philipson for providing us with anti-NCX1 and anti-NCX3 antibodies; Heart and Stroke Foundation & Manitoba Health Research Council for research funding to RB; Canadian Diabetes Association, Novo Nordisk Canada Inc. for a Doctoral Student Research Award to DER.

## Conflict of interest

None.

## References

Alexander SP, Mathie A, Peters JA (2011). Guide to receptors and channels (GRAC), 5th edition. Br J Pharmacol 164 (Suppl. 1): S1–S324.

Alkon DL, Rasmussen H (1988). A spatial-temporal model of cell activation. Science 239: 998–1005.

Authi KS, Crawford N (1985). Inositol 1,4,5-trisphosphate-induced release of sequestered Ca2+ from highly purified human platelet intracellular membranes. Biochem J 230: 247–253.

Baumgartner HR, Haudenschild C (1972). Adhesion of platelets to subendothelium. Ann N Y Acad Sci 201: 22–36.

Born GV (1972). Current ideas on the mechanism of platelet aggregation. Ann N Y Acad Sci 201: 4–12.

Brass LF, Joseph SK (1985). A role for inositol triphosphate in intracellular Ca2+ mobilization and granule secretion in platelets. J Biol Chem 260: 15172–15179.

Cervetto L, Lagnado L, Perry RJ, Robinson DW, McNaughton PA (1989). Extrusion of calcium from rod outer segments is driven by both sodium and potassium gradients. Nature 337: 740–743.

Cowan DH, Robertson AL, Shook P, Giroski P (1981). Platelet adherence to collagen: role of plasma, ADP, and divalent cations. Br J Haematol 47: 257–267.

Eder P, Probst D, Rosker C, Poteser M, Wolinski H, Kohlwein SD *et al.* (2007). Phospholipase C-dependent control of cardiac calcium homeostasis involves a TRPC3-NCX1 signaling complex. Cardiovasc Res 73: 111–119.

Enyedi A, Sarkadi B, Foldes-Papp Z, Monostory S, Gardos G (1986). Demonstration of two distinct calcium pumps in human platelet membrane vesicles. J Biol Chem 261: 9558–9563.

Flores-Soto E, Carbajal V, Reyes-Garcia J, Garcia-Hernandez LM, Figueroa A, Checa M *et al.* (2011). In airways ATP refills sarcoplasmic reticulum via P2X smooth muscle receptors and induces contraction through P2Y epithelial receptors. Pflugers Arch 461: 261–275.

Fung CY, Brearley CA, Farndale RW, Mahaut-Smith MP (2005). A major role for P2X1 receptors in the early collagen-evoked intracellular Ca2+ responses of human platelets. Thromb Haemost 94: 37–40.

Gabellini N, Bortoluzzi S, Danieli GA, Carafoli E (2002). The human SLC8A3 gene and the tissue-specific Na+/Ca2+ exchanger 3 isoforms. Gene 298: 1–7.

Grette K (1962). Studies on the mechanism of thrombin-catalyzed hemostatic reactions in blood platelets. Acta Physiol Scand Suppl 195: 1–93.

Grynkiewicz G, Poenie M, Tsien RY (1985). A new generation of Ca2+ indicators with greatly improved fluorescence properties. J Biol Chem 260: 3440–3450.

Gudermann T, Hofmann T, Mederos y Schnitzler M, Dietrich A (2004). Activation, subunit composition and physiological relevance of DAG-sensitive TRPC proteins. Novartis Found Symp 258: 103–118; discussion 118–122, 155–109, 263–106.

Harper AG, Sage SO (2007a). A key role for reverse Na+/Ca2+ exchange influenced by the actin cytoskeleton in store-operated Ca2+ entry in human platelets: evidence against the de novo conformational coupling hypothesis. Cell Calcium 42: 606–617.

Harper AG, Sage SO (2007b). A role for the intracellular protease calpain in the activation of store-operated calcium entry in human platelets. Cell Calcium 41: 169–178.

Harper AG, Mason MJ, Sage SO (2009). A key role for dense granule secretion in potentiation of the Ca2+ signal arising from store-operated calcium entry in human platelets. Cell Calcium 45: 413–420.

Harper MT, Mason MJ, Sage SO, Harper AG (2010). Phorbol ester-evoked Ca2+ signaling in human platelets is via autocrine activation of P(2X1) receptors, not a novel non-capacitative Ca2+ entry. J Thromb Haemost 8: 1604–1613.

Hechler B, Lenain N, Marchese P, Vial C, Heim V, Freund M *et al.* (2003). A role of the fast ATP-gated P2X1 cation channel in thrombosis of small arteries in vivo. J Exp Med 198: 661–667.

Heptinstall S (1976). The use of a chelating ion-exchange resin to evaluate the effects of the extracellular calcium concentration on adenosine diphosphate induced aggregation of human blood platelets. Thromb Haemost 36: 208–220.

Hinata M, Kimura J (2004). Forefront of Na+/Ca2+ exchanger studies: stoichiometry of cardiac Na+/Ca2+ exchanger; 3:1 or 4:1? J Pharmacol Sci 96: 15–18.

Iwamoto T, Watano T, Shigekawa M (1996). A novel isothiourea derivative selectively inhibits the reverse mode of Na+/Ca2+ exchange in cells expressing NCX1. J Biol Chem 271: 22391–22397.

Iwamoto T, Kita S, Zhang J, Blaustein MP, Arai Y, Yoshida S *et al.* (2004). Salt-sensitive hypertension is triggered by Ca2+ entry via Na+/Ca2+ exchanger type-1 in vascular smooth muscle. Nat Med 10: 1193–1199.

Jy W, Haynes DH (1987). Thrombin-induced calcium movements in platelet activation. Biochim Biophys Acta 929: 88–102.

Kimura M, Aviv A, Reeves JP (1993). K(+)-dependent Na+/Ca2+ exchange in human platelets. J Biol Chem 268: 6874–6877.

Kimura M, Jeanclos EM, Donnelly RJ, Lytton J, Reeves JP, Aviv A (1999). Physiological and molecular characterization of the Na+/Ca2+ exchanger in human platelets. Am J Physiol 277 (3 Pt 2): H911–H917.

Lewandrowski U, Wortelkamp S, Lohrig K, Zahedi RP, Wolters DA, Walter U *et al.* (2009). Platelet membrane proteomics: a novel repository for functional research. Blood 114: e10–e19.

Li Y, Woo V, Bose R (2001). Platelet hyperactivity and abnormal Ca(2+) homeostasis in diabetes mellitus. Am J Physiol Heart Circ Physiol 280: H1480–H1489.

Li Z, Matsuoka S, Hryshko LV, Nicoll DA, Bersohn MM, Burke EP *et al.* (1994). Cloning of the NCX2 isoform of the plasma membrane Na(+)-Ca2+ exchanger. J Biol Chem 269: 17434–17439.

Linck B, Qiu Z, He Z, Tong Q, Hilgemann DW, Philipson KD (1998). Functional comparison of the three isoforms of the Na+/Ca2+ exchanger (NCX1, NCX2, NCX3). Am J Physiol 274 (2 Pt 1): C415–C423.

MacIntyre DE, Rink TJ (1982). The role of platelet membrane potential in the initiation of platelet aggregation. Thromb Haemost 47: 22–26.

Matsuda T, Arakawa N, Takuma K, Kishida Y, Kawasaki Y, Sakaue M *et al.* (2001). SEA0400, a novel and selective inhibitor of the Na+-Ca2+ exchanger, attenuates reperfusion injury in the in vitro and in vivo cerebral ischemic models. J Pharmacol Exp Ther 298: 249–256.

Morton LF, Peachey AR, Barnes MJ (1989). Platelet-reactive sites in collagens type I and type III. Evidence for separate adhesion and aggregatory sites. Biochem J 258: 157–163.

Nicoll DA, Longoni S, Philipson KD (1990). Molecular cloning and functional expression of the cardiac sarcolemmal Na(+)-Ca2+ exchanger. Science 250: 562–565.

Nicoll DA, Quednau BD, Qui Z, Xia YR, Lusis AJ, Philipson KD (1996). Cloning of a third mammalian Na+-Ca2+ exchanger, NCX3. J Biol Chem 271: 24914–24921.

Nishizuka Y (1984). The role of protein kinase C in cell surface signal transduction and tumour promotion. Nature 308: 693–698.

Oury C, Toth-Zsamboki E, Vermylen J, Hoylaerts MF (2002). P2X(1)-mediated activation of extracellular signal-regulated kinase 2 contributes to platelet secretion and aggregation induced by collagen. Blood 100: 2499–2505.

Oury C, Kuijpers MJ, Toth-Zsamboki E, Bonnefoy A, Danloy S, Vreys I *et al.* (2003). Overexpression of the platelet P2X1 ion channel in transgenic mice generates a novel prothrombotic phenotype. Blood 101: 3969–3976.

Papp B, Enyedi A, Kovacs T, Sarkadi B, Wuytack F, Thastrup O *et al.* (1991). Demonstration of two forms of calcium pumps by thapsigargin inhibition and radioimmunoblotting in platelet membrane vesicles. J Biol Chem 266: 14593–14596.

Pfaffl MW (2001). A new mathematical model for relative quantification in real-time RT-PCR. Nucleic Acids Res 29: e45.

Pipili E (1985). Platelet membrane potential: simultaneous measurement of diSC3(5) fluorescence and optical density. Thromb Haemost 54: 645–649.

Poole AW, Watson SP (1995). Regulation of cytosolic calcium by collagen in single human platelets. Br J Pharmacol 115: 101–106.

Quednau BD, Nicoll DA, Philipson KD (1997). Tissue specificity and alternative splicing of the Na+/Ca2+ exchanger isoforms NCX1, NCX2, and NCX3 in rat. Am J Physiol 272 (4 Pt 1): C1250–C1261.

Reeves JP, Hale CC (1984). The stoichiometry of the cardiac sodium-calcium exchange system. J Biol Chem 259: 7733–7739.

Rengasamy A, Soura S, Feinberg H (1987). Platelet Ca2+ homeostasis: Na+-Ca2+ exchange in plasma membrane vesicles. Thromb Haemost 57: 337–340.

Rink TJ, Smith SW, Tsien RY (1982). Cytoplasmic free Ca2+ in human platelets: Ca2+ thresholds and Ca-independent activation for shape-change and secretion. FEBS Lett 148: 21–26.

Rittenhouse SE, Allen CL (1982). Synergistic activation by collagen and 15-hydroxy-9 alpha,11 alpha-peroxidoprosta-5,13-dienoic acid (PGH2) of phosphatidylinositol metabolism and arachidonic acid release in human platelets. J Clin Invest 70: 1216–1224.

Roberts DE, Bose R (2002). Reverse mode Na+/Ca2+ exchange in the collagen activation of human platelets. Ann N Y Acad Sci 976: 345–349.

Roberts DE, McNicol A, Bose R (2004). Mechanism of collagen activation in human platelets. J Biol Chem 279: 19421–19430.

Roberts D, Richman-Eisenstat J, Bose R (2005). Characterization of the human platelet Na+/Ca2+ exchanger. FASEB J 19 (4 Pt 1): A679–A680.

Rosker C, Graziani A, Lukas M, Eder P, Zhu MX, Romanin C *et al.* (2004). Ca(2+) signaling by TRPC3 involves Na(+) entry and local coupling to the Na(+)/Ca(2+) exchanger. J Biol Chem 279: 13696–13704.

Rozen S, Skaletsky H (2000). Primer3 on the WWW for general users and for biologist programmers. Methods Mol Biol 132: 365–386.

Schaeffer J, Blaustein MP (1989). Platelet free calcium concentrations measured with fura-2 are influenced by the transmembrane sodium gradient. Cell Calcium 10: 101–113.

Schnetkamp PP, Basu DK, Szerencsei RT (1989). Na+-Ca2+ exchange in bovine rod outer segments requires and transports K+. Am J Physiol 257 (1 Pt 1): C153–C157.

Takano S, Kimura J, Ono T (2001). Inhibition of aggregation of rabbit and human platelets induced by adrenaline and 5-hydroxytryptamine by KB-R7943, a Na(+)/Ca(2+) exchange inhibitor. Br J Pharmacol 132: 1383–1388.

Tanaka H, Nishimaru K, Aikawa T, Hirayama W, Tanaka Y, Shigenobu K (2002). Effect of SEA0400, a novel inhibitor of sodium-calcium exchanger, on myocardial ionic currents. Br J Pharmacol 135: 1096–1100.

Valera S, Hussy N, Evans RJ, Adami N, North RA, Surprenant A *et al.* (1994). A new class of ligand-gated ion channel defined by P2x receptor for extracellular ATP. Nature 371: 516–519.

Watson SP, Reep B, McConnell RT, Lapetina EG (1985). Collagen stimulates [3H]inositol trisphosphate formation in indomethacin-treated human platelets. Biochem J 226: 831–837.

Wuytack F, Papp B, Verboomen H, Raeymaekers L, Dode L, Bobe R *et al.* (1994). A sarco/endoplasmic reticulum Ca(2+)-ATPase 3-type Ca2+ pump is expressed in platelets, in lymphoid cells, and in mast cells. J Biol Chem 269: 1410–1416.